ZEOLITE/CHITOSAN/GELATIN FILMS: PREPARATION, SUPERCRITICAL CO_2 PROCESSING, CHARACTERIZATION AND BIOACTIVITY

Jelena Pajnik[1], Jelena Dikić[1], Stoja Milovanovic[2], Milena Milosevic[3], Sanja Jevtic[2], Ivana Lukić[2]*

[1]University of Belgrade, Innovation Centre of the Faculty of Technology and Metallurgy, Karnegijeva 4, 11120 Belgrade, Serbia

[2]University of Belgrade, Faculty of Technology and Metallurgy, Karnegijeva 4, 11120 Belgrade, Serbia

[3]University of Belgrade, Institute of Chemistry, Technology and Metallurgy, Njegoševa 12, 11000 Belgrade, Serbia

Highlights

- SSI process enabled preparation of composites effective against *E. coli* and *S. aureus.*
- Antioxidant activity of the composite films was greatly improved after the SSI.
- Thymol/carvacrol loaded films expressed initial burst release during first 6 h in PBS.
- Thermal properties of the films were improved after the SSI process.

Table of Contents (ToC)

Chitosan/gelatin and chitosan/gelatin/zeolite films loaded with thymol/carvacrol in supercritical CO_2 are proven to possess antibacterial and antioxidant properties. After initial burst during first 6 h of the test, loaded materials exhibits gradual release of active compounds. Solubility of films in water is low, while water vapor transmission rate (> 76 gm^{-2} day^{-1}) confirms that prepared composites are suitable for wound dressing application.

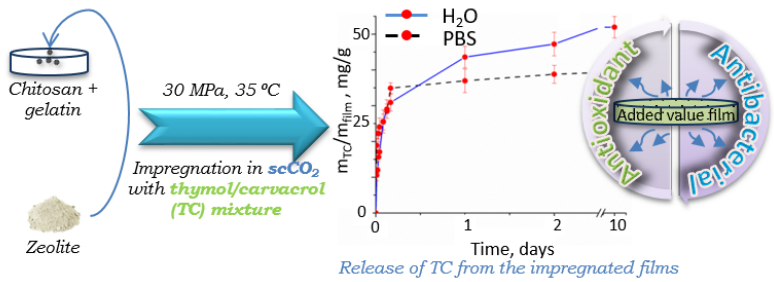

Release of TC from the impregnated films

ABSTRACT

This article has been accepted for publication and undergone full peer review but has not been through the copyediting, typesetting, pagination and proofreading process, which may lead to differences between this version and the Version of Record. Please cite this article as doi: 10.1002/mame.202200009.

Chitosan/gelatin and chitosan/gelatin/zeolite films prepared by solvent casting method were impregnated with a mixture of thymol and carvacrol using a green solvent, supercritical carbon dioxide at 35 °C and 30 MPa, during 18 h. Proposed method enabled preparation of biocompatible and biodegradable blends with strong antioxidant and antibacterial activity, whereby amounts of loaded thymol/carvacrol mixture were in the range from 3.3-6%. After initial burst release, both types of films exhibited gradual release of bioactive compounds, with around 72 and 96% of impregnated thymol/carvacrol mixture released in water and PBS (pH 7.4) during tested period of 10 days, respectively. Results of water vapor transmission rate (> 76 gm^{-2} day^{-1}) confirmed that prepared composites are suitable for wound dressing application. Thermal analysis showed superior properties of prepared thymol/carvacrol loaded films compared to control samples. In addition, mechanical and structural properties, as well as solubility and swelling behavior of the obtained films were investigated in detail.

Keywords: Biopolymer; Processing; $scCO_2$; Impregnation; Thymol.

---

*Corresponding author: E-mail address: jpajnik@tmf.bg.ac.rs

INTRODUCTION

Plants produce a variety of compounds that have significant role in its protection against different pathogens [1]. Some of these natural compounds, that exhibit antimicrobial properties, are usually present in plant essential oils as a mixture of volatile secondary metabolites [2]. Among them, phenols and polyphenols are the most studied as they also express antimicrobial activity against human pathogens [3,4]. Two major phenolic compounds of oregano (*Origanum vulgare*) and thyme (*Thymus vulgaris*) oils are thymol [2-Isopropyl-5-methylphenol] and carvacrol [5-Isopropyl-2-methylphenol]. Both thymol and carvacrol have been used in traditional medicine since ancient times [5]. They possess a variety of biological properties such as antimicrobial, antioxidant, anti-inflammatory, antitumor, anti-mutagen, analgesic, anti-parasitic and insecticidal [5,6]. The susceptibility of methicillin resistant *Staphylococcus aureus* (MRSA) to carvacrol and thymol was also proven [7]. Furthermore, it was reported that thymol and carvacrol in a mixture exhibit synergetic activity enabling desired antimicrobial and antioxidant activity at lower concentrations compared to their individual performances [8,9]. In addition, United States Food and Drug Administration (FDA) has generally recognized thymol and carvacrol as safe [10]. In order to preserve these active compounds from evaporation and environmental effects and to enable their gradual release at

specific site, loading of thymol/carvacrol mixture into biocompatible and biodegradable polymers was explored in this study.

Loading of active substances into polymer carriers in most cases implies utilization of aqueous or organic solutions, depending on an active substance and polymer solubility, solvent toxicity and capability of solvent to be removed [11]. Despite simplicity of conventional methods for incorporation of desirable compounds into polymer matrixes, some disadvantages must be pointed out such as utilization of toxic organic solvents in some cases, undesired reactions, photochemical and thermal degradation, low incorporation, non-unique dispersion of an active substance, additional step of material drying, solvent residue in final material, etc. [11]. On the other hand, application of supercritical solvent impregnation (SSI) as a technique for loading of desirable compounds into polymer network offers a possibility to overcome aforementioned challenges [12,13]. Supercritical carbon dioxide ($scCO_2$) is the green solvent most commonly used in SSI process as it provides high diffusivity into organic matter due to low viscosity and near zero surface [14,15]. In addition, this process enables final product, without solvent residues, obtained by simple depressurization of the system [13].

Various solid carriers were reported as suitable for SSI with bioactive agents. For example, metal-organic frameworks were impregnated with carvacrol [16], cellulose acetate was impregnated with thymol [17] and pyrethrum extract [18], gelatin-chitosan was impregnated with clove essential oil [19], poly(D,L-lactic acid) [20], poly(D,L-lactic-co-glycolic acid) [21], poly(D,L-lactic acid)/poly(ε-caprolactone) [22], LDPE nanocomposites [23] and starch [14] were impregnated with thymol. However, there is only one report in available literature that describes utilization of SSI process for loading of thymol/carvacrol mixture into poly(D,L-lactic acid)/poly(ε- caprolactone) [24].

In this study, thymol/carvacrol mixture was loaded into composite films composed of chitosan and gelatin using SSI process. Both of this polymers, obtained from natural and renewable resources, are biodegradable, non-toxic and biocompatible [25]. In addition, it was previously reported that chitosan and gelatin promote wound healing which makes them perfect materials for wound dressing application [26,27]. Also, recent reports pointed out improved activity of composites obtained by combination of chitosan and gelatin [25]. In order to improve properties of prepared chitosan/gelatin films and to improve its loading capacity, addition of highly porous zeolite was also proposed. Zeolites themselves are also considered as effective carriers for different compounds as they can exhibit controlled release [28–31]. Our previous research showed the possibility of impregnation of chitosan/starch/zeolite composites with thymol using $scCO_2$ [32]. However, to the

best of our knowledge, this manuscript presents application of SSI process for loading of thymol/carvacrol mixture into chitosan/gelatin and chitosan/gelatin/zeolite films for the first time. Additionally, antibacterial and antioxidant activity, along with structural, thermal and mechanical properties of the obtained composites were discussed in detail.

EXPERIMENTAL

2.1. Materials

High molecular weight chitosan (310000-375000 g/mol, 75–85% deacetylated), gelatin from bovine skin, thymol (purity > 99 %) and carvacrol (purity > 99.0 %) were purchased from Sigma-Aldrich Chemie GmbH, (Steinheim, Germany). Commercial CO_2 (purity 99.9%) was supplied by Messer–Tehnogas (Serbia), sodium chloride (p.a. grade) was obtained from Sigma-Aldrich Chemie GmbH (Germany) and ethanol (99.9%) was purchased from Merck Millipore (Germany). The natural zeolite tuff, which contained about 70 wt.% of clinoptilolite (quartz and anorthite were major impurities), was obtained from Slanci deposit (Serbia). 1,1-diphenyl-2-picryldrazil ($DPPH^{\bullet}$), 2,2'-azino-bis(3-ethylbenzothiazoline-6-sulfonic acid) ($ABTS^{\bullet+}$), potassium persulfate and salts for phosphate buffered solution (sodium chloride, potassium chloride, sodium hydrogenphosphate and potassium dihydrogen phosphate) were purchased from Sigma-Aldrich Chemie GmbH (Steinheim, Germany). Methanol was obtained from Acros Organics (Geel, Belgium).

2.2. Preparation of zeolite sample

Zeolitic tuff from Slanci deposit (Serbia) containing about 70 wt% of natural zeolite – clinoptilolite with particle size of 63-125 μm was used. Specific surface area of the zeolite was enlarged by procedure previously published [33]. In short, the procedure consists of firstly transforming the Z into NH_4-form (NH_4-Z) by treatment with a solution of ammonium acetate (1 mol dm^{-3}) during 24 h at room temperature. Further, NH_4-Z was calcinated in the air at 550 ºC for 3 h and then calcined product was treated with 0.6 mol dm^{-3} of HCl at 70 ºC for 1 h. Subsequently, the obtained solid was treated with fresh 0.05 mol dm^{-3} of HCl and ultrasound (Bandelin, Sonopuls) three times. Solid was than rinsed in distilled water until the negative reaction to chloride ions and dried at 60 ºC to a constant mass. The final product was denoted as Z.

2.3. Preparation of blends

Chitosan was dissolved in a 2% (w/v) acetic acid solution to yield a 2% (w/v) chitosan suspension. The suspension was stirred using a magnetic stirrer until the clear solution was obtained. The 2% (w/v) gelatin solution was prepared by dispersing the gelatin in distilled water and heating the

suspension on a hotplate for 20 min at 80 °C with stirring. Chitosan/gelatin (CG) films were prepared by mixing the chitosan solution (2% w/v) with the gelatin solution (2% w/v) in mass ratio of 1:1. Glycerol (25% w/w of the total solid weight) was added to the mixture. The mixture was stirred at 80 °C for 40 min using a magnetic stirrer and subsequently cooled to the room temperature. The obtained mixture was casted onto the plastic molds (12 cm diameter). After drying at room temperature for 24 h, the films were additionally dried in an oven over night at 35 °C. Obtained sample was denoted as CG (1-0).

CG films containing zeolite were prepared as follows. An amount of 30% (w/w) of zeolite (based on the total solid weight) was added during the mixing step of chitosan and gelatin solutions. Afterwards, the suspension was vigorously stirred (15000 rpm) for 15 min using an Ika Ultra-Turrax disperser (Staufen, Germany). The subsequent steps of casting the obtained suspension and drying were conducted as previously described. Obtained sample was denoted as CGZ (2-0).

2.4. Supercritical impregnation

The prepared CG (1-0) and CGZ (2-0) films were impregnated with thymol/carvacrol (TC) mixture in $scCO_2$ at 30 MPa, 35 ºC for 18 h. These conditions employed in our previous study [32] were found as optimum for functionalization of starch/chitosan/zeolite films with thymol. The experiments were conducted in a high-pressure view chamber (Eurotechnica GmbH, Germany), using a static method, as previously described [17,32,34]. The initial mass ratio of thymol/carvacrol mixture to films in the view chamber was 10/1, while mass ratio of thymol to carvacrol in the mixture was 1:1. The decompression rate, applied at the end of SSI process, was 1.5 MPa/min. TC impregnated 1-0 and 2-0 samples were denoted as 1-1 and 2-1, respectively.

The amount of loaded thymol/carvacrol mixture in the films was determined after complete disintegration/solubilisation of the samples in the 2% acetic solution (100 ml) by measuring of absorbance at 276 nm [24] using a UV-Vis spectrophotometer (Shimadzu 1700).

2.5. Antibacterial activity

The antibacterial activity of prepared films was tested towards Gram-negative bacterium *Escherichia coli* strain DSM 498 and Gram-positive bacterium *Staphylococcus aureus* strain ATCC 25923. Bacteria were pre-grown on the Nutrient agar (NA, Torlak, Serbia) for 16 h at 37±0.1 ºC to obtain cultures in a *log* phase of growth.

The disk diffusion method was used for the qualitative assessment of the antibacterial activity. Prior to test, all prepared films were sterilized by UV light for 30 min. Biomass of each bacterial strain was

separately suspended in a sterile physiological solution to obtain bacterial concentration of about 10^9 CFU/mL. Agar diffusion test was performed on Mueller Hinton agar (MH, Torlak, Serbia). First, the bacteria biomass was inoculated on the agar, and then sterile films, cut into pieces of 1 cm^2, were placed on agar plate. The plates were incubated for 24 h at 37 ºC. After incubation, the clear zones without bacteria growth around films were inspected visually. Antibacterial activity of the TC loaded composites was compared with neat films as control.

2.6. Antioxidant activity

2.6.1. DPPH free radical scavenging assay

Slight modifications of the method [35] of 2,2-diphenyl-1-picrylhydrazyl radical ($DPPH^{\bullet}$) assay was applied to test antioxidant activity of the prepared films before and after the SSI. In general, 1 mg of the control and TC impregnated films were soaked in 100 mL of distilled water or Phosphate Buffered Saline solution (PBS, pH 7.4). Subsequently, samples (volume of 0.3 mL) of solutions were taken each 10 minutes for 1.5 h and after 2 h and 24 h. Each extract solution was mixed with 2.8 mL $DPPH^{\bullet}$ radical solution in methanol (7mM). The 0.3 mL of mixture of pure distilled water/PBS solution and 2.8 mL $DPPH^{\bullet}$ were used as a control. In addition, the scavenging activity of 0.3 mL of TC mixture (mass ratio of T/C was 1/1) in 2.8 mL $DPPH^{\bullet}$ was evaluated as well. After incubation of 30 min at room temperature, absorbance value was determined at 517 nm. Ascorbic acid was used as a reference standard. All the measurements were performed in triplicate, and the scavenging activity was calculated using equation (1):

$$\text{Scavenging activity} = \frac{(A_{control} - A_{sample})}{A_{control}} \cdot 100 \quad (1)$$

where A_{sample} and $A_{control}$ refer to the absorbance of $DPPH^{\bullet}$ radical in the sample and control solutions, respectively.

2.6.2. ABTS free radical scavenging assay

The 2,2'-azino-bis(3-ethylbenzothiazoline-6-sulfonic acid) (ABTS) assay was performed using the literature method [36] with slight modifications. Firstly, $ABTS^{\bullet+}$ radical cation solution was prepared by mixing ABTS stock solution (7.8 mM) and potassium persulfate ($K_2S_2O_8$) solution (2.45 mM). Afterwards, prepared solution was left 12-16 h in a dark for completion of a reaction, and then solution was diluted with methanol to obtain absorbance of 0.700±0.020 at 734 nm. The solutions with film sample were prepared as in DPPH assay. The 0.3 mL of each sample solution was added to 2.8 mL of $ABTS^{\bullet+}$ solutions. The 0.3 mL of pure distilled water/PBS solution in 2.8 mL $ABTS^{\bullet+}$ were

used as controls. As in DPPH assay, antioxidant activity of TC mixture was determined as well. The 0.3 mL of the TC mixture were mixed with 2.8 mL $ABTS^{\bullet+}$. The distilled water or PBS without antioxidant as control was also prepared. Absorbance at 734 nm of all sample was determined after incubating in the dark for 30 min at room temperature. Ascorbic acid was used as a reference standard. This test was carried out in triplicate. The scavenging activity was calculated using Eq.1, where A_{sample} and $A_{control}$ refer to the absorbance of $ABTS^{\bullet+}$ in the sample and control solutions, respectively.

2.7. Release kinetics

Kinetic study on TC release from the impregnated films in both deionized water (25 °C) and PBS (pH 7.4) at 37 °C was performed using a UV-Vis spectrophotometer (Shimadzu 1800, Japan) at 276 nm. Film samples (0.0022±0.0005 g) were immersed in 100 ml of distilled water/PBS without stirring. At pre-determined periods, an aliquot (3.5 ml) of the solution was taken, analyzed and then returned into the release medium. Release experiments were carried out in duplicate during 10 days. TC concentration was calculated using a previously determined calibration curve. Experimental results were given as released mass of TC mixture per g of impregnated film plotted against time.

Two kinetic models, Weibull (Eq. 2) and Higuchi (Eq. 3) were used to fit the experimental data:

Weibull:
$$\frac{M_t}{M_\infty} = 1 - \exp(-a \cdot t^b) \quad (2)$$

Higuchi:
$$\frac{M_t}{M_\infty} = k_H \cdot t^{1/2} \quad (3)$$

where M_t is the amount of TC released at time t, M_∞ is the amount of TC loaded in the film; a and b are constants. The nonlinear regression module of Polymath Educational 6.10 software package was used to determine parameters of the models used.

2.8. Characterization of the samples

2.8.1. FTIR analysis

Fourier-transform infrared (FTIR) spectra of films impregnated with TC mixture as well as neat films were recorded in the ATR mode using a Nicolet™ iS™ 10 Spectrometer (Thermo

Fisher SCIENTIFIC) with a resolution of 4 cm^{-1} at wavenumbers in the range of 4000-500-cm^{-1}.

2.8.2. Scanning electron microscopy (SEM) analysis

The surface morphology of the 1-0 and 2-0 samples before and after the SSI with TC mixture was analyzed by field emission scanning electron microscopy (JEOL JSM-6610LV). The samples were coated with a thin layer of gold before the analysis.

2.8.3. TGA-DTG analysis

Thermal properties of the prepared films were investigated by thermogravimetric and derivative thermogravimetric analysis (TGA-DTG) using a SDT Q600 simultaneous TGA-DTA instrument (TA Instruments). The samples were heated in a standard alumina sample pan from room temperature up to 600 °C at a heating rate of 10 °C min^{-1} under nitrogen atmosphere with a flow rate of 100 cm^3 min^{-1}.

2.8.4. Water vapor permeability

Water vapor permeability (WVP) measurements were conducted according to the standardized methodology [37,38]. Measurements were carried out gravimetrically at 25 °C and 75% relative humidity (RH) in the desiccator (Star desiccator, Bela). Saturated sodium chloride was used to provide desired RH in the desiccator. The samples were sealed over a circular opening (exposed area of 12.56 cm^2) of aluminum permeation cells filled with anhydrous sodium chloride to provide 0% RH inside the cell and placed inside the desiccator. Due to the moisture gradient, water vapor penetrates through the tested samples towards the inside of the cells, while anhydrous sodium chloride soaks up water vapor, which results in a weight increase of the cells. The cells' weight change was determined twice a day for seven days, using an analytical scale with an accuracy of ±0. 1 mg. Tests were run in triplicates.

Changes in the weight of the cells were plotted with respect to time, and the linear least-square method was used for the calculation of the parameters given by Eqs.5 and 6 [39,40] :

$$WVTR = \frac{\Delta m}{t \cdot A} \tag{5}$$

$$WVP = \frac{L \cdot WVTR}{\Delta p} \tag{6}$$

where *WVTR* is the water vapor transmission rate of films (g/s), *L* is average thickness of the film (m), *A* is the permeation area (m^2), Δp is the difference in water vapor pressure between the two exposed sides of the film (Pa).

2.8.5. Water solubility of films

Solubility of films was determined as follows. Specimens of films (2x2 cm) were dried in an oven at 105 °C during 24 h and initial dry weight (W_i) was determined using analytical scale (±0.0001 g). Afterwards, dried samples were immersed into 30 mL of distilled water and placed inside the incubator (Colo, IN1017, Slovenia) at 25 °C for 24 h. After this period, films were taken out from water and dried once again in an oven at 105 °C during 24 h and remaining mass of samples (W_f) was determined. Solubility of films (S%) was determined using following formula [41,42]:

$$S(\%) = \frac{W_i - W_f}{W_i} \cdot 100 \quad (7)$$

The cross-linking or weight remaining percentage was calculated using following formula [43]:

$$Cross-linking(\%) = \frac{W_f}{W_i} \cdot 100 \quad (8)$$

All tests are the means of at least 3 measurements.

2.8.6. Swelling test of films

Samples were dried to a constant weight prior swelling analysis in an oven at 105 °C for 24 h. Films' specimens were immersed into 50 mL of PBS (pH 7.4). The flasks containing PBS and samples were kept at temperature of 37 °C for the duration of swelling experiment (24 h) in a water bath (Memmert WNB 22, Slovenia) with gentle stirring. The sample were taken out from the flasks after 1, 4, 6 and 24 h, wiped between filter papers to remove the excess of moisture and weighed (W_t).

The swelling percentage (SW%) was calculated using the following equation [44]:

$$SW(\%) = \frac{W_t - W_i}{W_i} \cdot 100 \quad (9)$$

All tests were performed in triplicates.

2.8.4. Mechanical analysis

Mechanical properties of the films were tested using AGS-X testing machine (Shimadzu, Japan) at room temperature (22 °C). Tensile testing was performed at 2 mm/min crosshead speed. Tensile strength as tensile stress at break and percent elongation at break were calculated from tension data. Young's modulus was calculated as a slope of initial linear portion of stress–strain curve. Three specimens of each film were tested and average values were reported.

RESULTS

3.1. SSI of composite films with thymol/carvacrol mixture

SSI process was performed in order to functionalize previously prepared CG and CGZ films with bioactive components. The results showed that SSI method was efficient for delivering of TC mixture into the prepared CG (1-0) and CGZ (2-0) films at selected conditions of 30 MPa and 35 °C during 18 h. The amount of loaded TC in the CG (1-0) was 3.3% (i.e. 36.1 mg_{TC}/g_{film}). Higher loading capacity of CG films were previously reported when clove oil was used [19]. Namely, depending on the SSI process conditions (40 °C, 10-30 MPa, 2-18 h), amounts of loaded clove oil in the CG films were in the range from 50-130 mg/g [19]. The difference in the loading values between reported findings and results of this study can be explained by the differences in process conditions. Namely, process pressure, temperature, operating time, and decompression rate greatly influence polymer impregnation. In addition, the efficiency of the SSI is greatly influenced by the partition coefficient of solute (active substance) between the polymer and the supercritical fluid phase, plasticizing effect of supercritical solution (CO_2 and the solute), and the existence of specific interactions between $scCO_2$ and/or solute with the polymer network [19,45,46]. This conclusion is also supported by the findings of Lukic et al. [24] who reported that poly(lactic acid)/poly(*ε*-caprolactone) film can be loaded with TC mixture in the amount of 215 mg_{TC}/g_{film} at 40 °C and 10 MPa during 5 h [24].

Results of proposed SSI process also revealed that CGZ (2-0) film was impregnated with almost 70% higher amount of TC mixture (6.0% i.e. 54.2 mg_{TC}/g_{film}) compared to the loading of CG film. Increase of loading capacity of the film with addition of zeolite is in accordance with the results from our previous study, where incorporation of zeolite into the starch/chitosan blend increased the sorption capacity of the material towards thymol greatly [32]. The reason for this can be found in the high porosity of zeolite and relatively high affinity of zeolite towards thymol and carvacrol in $scCO_2$-assisted process [47].

In order to investigate biological activity of prepared materials, antibacterial and antioxidant

activity was further tested. TC impregnated samples with and without zeolite were denoted as 2-1 and 1-1, respectively.

3.2. Antibacterial properties of the obtained films

The antibacterial activity of prepared films, with and without bioactive components, is shown in Fig 1. It is evident that both control samples (with and without zeolite) did not exhibit antibacterial activity towards tested bacteria stains. This result is in accordance with the literature, which reports that neither gelatin/chitosan film [48], nor zeolite [49,50] itself exhibit antibacterial activity.

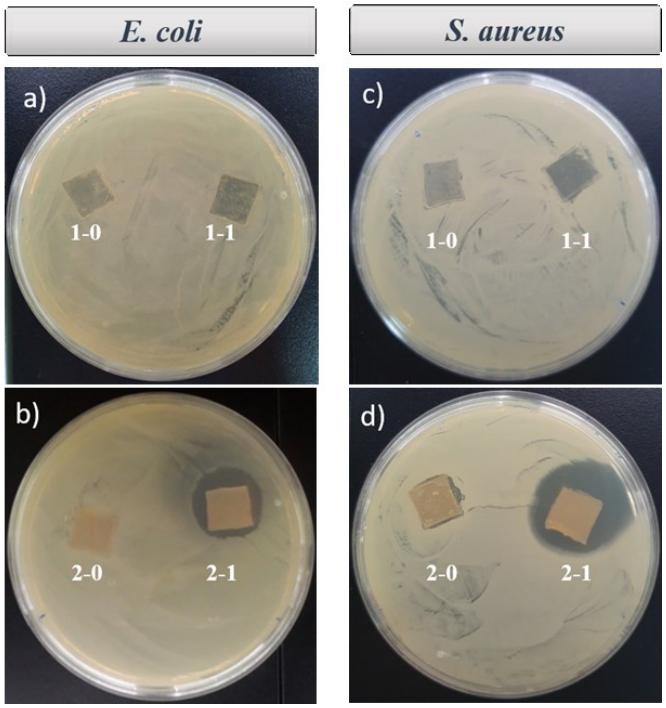

Fig. 1 Antibacterial activity of the control (1-0; 2-0) and TC impregnated films (1-1; 2-1) towards *E. coli (a* and *b)* and *S. aureus (c* and *d)*. Initial number of bacteria (t_0, CFU/mL): *E. coli* = $7.15 \cdot 10^9$; *S. aureus* = $1.4 \cdot 10^9$

Antibacterial effect of 1-1 sample was insignificant and slightly more pronounced in contact with *S. aureus* (Fig. 1a,c). On the other hand, 2-1 sample exhibited strong antibacterial activity towards both bacterial stains (Fig. 1b,d). The reason for different antimicrobial activity toward tested bacteria can be found in amount of loaded TC mixture. Namely, the higher loadings of natural bioactive compound, the stronger antimicrobial activity will be [17,51]. CGZ impregnated film (2-1) enabled formation of the zones of inhibition that have diameter of approximately 4 mm and 8 mm for *E. coli* and *S. aureus*, respectively. It is worth to notice that impregnated films showed higher activity towards Gram-positive bacteria strain. This observation can be explained by the structure of the cell wall of tested bacteria cells. Namely, outer membrane of the Gram-negative bacteria is composed

primarily of phospholipids and lipopolysaccharide molecules. This layer forms a hydrophilic permeability barrier which can serve as a protection against hydrophobic materials, such as thymol/carvacrol. In the case of Gram-positive bacteria like *S. aureus*, cell wall allows hydrophobic molecules to easily penetrate the cell and express its antibacterial effect [52]. The mechanism of the antibacterial activity of the phenols – thymol and carvacrol, is based on the interruption of the cell wall and membranes of the bacteria and it can lead to the cell lysis and the leaching of the cell content [53]. Thymol action is attributed to the integration of polar head-groups of the lipid bilayer which induce the alternation of the cell wall, whereas carvacrol action is linked to the presence of the hydroxyl group which acts as a trans-membrane carrier by carrying the H^+ ions into the cytoplasm and transporting K^+ ions back [54]. In addition, synergetic effect of carvacrol and thymol towards *E. coli* and *S. aureus* was previously reported [55].

3.3. Antioxidant activity of the films

High level reactive oxygen species (ROS) and free radical slow down the wound healing process. Therefore, natural biopolymers dressings possessing antioxidant capacity are highly desirable to reduce harmful effects of ROS [56]. Furthermore, it was proven that chitosan films incorporated with plants oils could be used as a potential wound healing materials [57]. The *in vitro* antioxidant scavenging activity of the control and TC impregnated films were determined using two free radical assays: DPPH and ABTS.

3.3.1. DPPH antioxidant assay

The results of *in vitro* antioxidant test for all prepared films are shown in Fig. 2 as a percent of inhibition of $DPPH^{\bullet}$ radical in relation to time. The control 1-0 sample showed negligible antioxidant activity (less than 1% of inhibition), while the activity of around 5% in the case of the control 2-0 film indicates that zeolite acts as possible source of dissolution of ion accelerating inhibition process. Previous study [58] showed that chitosan exhibit certain antioxidant potential depending on the molecular weight and the degree of deacetylation. Antioxidant efficiency was attributed to the presence of hydroxyl and protonated amino groups in its structure. Kyung et al. reported that large number of inter- and intra-molecular interaction between amino and hydroxyl groups in high molecular weight chitosan contribute to lower $DPPH^{\bullet}$ radical-scavenging activity [59]. Accordingly, the results from this study agree with low activity of control films. Additionally, amino acids, glycine and proline, present in the structure of gelatin, have donor groups that could react with $DPPH^{\bullet}$ free radical ccontributing to its stabilization [60]. Consequently,

the antioxidant activity of the control films could be attributed to the antioxidant activity of chitosan and gelatin. The interaction of electron-donating hydroxyl groups in the structure of both components of TC mixture, incorporated in both 1-0 and 2-0 films, with stable $DPPH^{\bullet}$ free radical led to significant increase of the measured antioxidant activity**,** in comparison to control samples. As can be seen from Fig. 2, the TC impregnated films (1-1, 2-1) showed moderate activity, with approximately up to 50% of inhibition after 60 min, compared to ascorbic acid. The activity slightly increased up to 70 min, and did not change after prolongation of the test to 2 h and 24 h. The TC mixture released from 1-1 film in water in the time range from 10 to 90 min showed antioxidant activity values from 0.7 to 35.5% (Figure 2a), while scavenging activity was in the range from 0.9 to 36.9% (Figure 2b) in the case of PBS medium. The TC mixture released from 2-1 film in the same time interval showed antioxidant activity in the range from 8.1 to 43.3% in water and from 8.5 to 45.6% in PBS medium (Figure 2a and b). These results reflect the significance of the time-dependent release of phenolic compounds from the impregnated carriers related to an antioxidative capabilities of release medium.

The literature reports indicate both hydrogen transfer (HAT) and single electron transfer (SET-PT) as possible mechanisms for antioxidant activity for phenolic-type compounds such as thymol and carvacrol [61]. Similarly, Ichikawa et al. reported SET-PT as a main radical scavenging mechanism for phenolic compounds in polar solvents such as water [62]. However, obtained results indicated the similarity between the used medium suggesting an analogous operative mechanism both in water and PBS, thus low dependence of radical scavenging activity on the properties of test solution.

Furthermore, it could be assumed that perceived antioxidant activity is a consequence of the quantity of released active molecules (effectiveness of film bonding to TC), and medium properties and electronic structure of antioxidant molecules (carvacrol and thymol) i.e. their electron/proton donating capability [63,64].

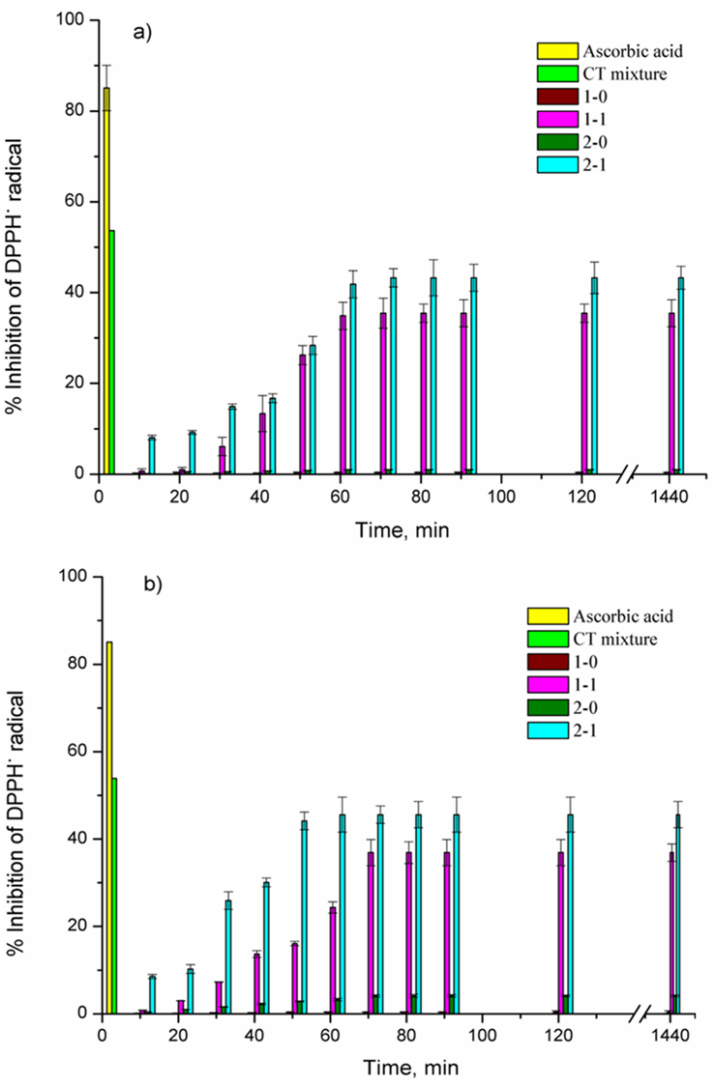

Fig. 2 Antioxidant activity of tested films a) in water and b) in PBS measured by DPPH• radical expressed as percent of inhibition

Literature reports that thymol loaded gelatin films expressed antioxidant activity in a dose-dependent manner, whereby antioxidant activity increased with increase of thymol amounts in the films [65]. Zhong et al. recently reported similar behavior of films prepared from peanut protein isolate impregnated with thymol (up to 2%)[66]. The highest DPPH scavenging activity of 22.47% was observed in the case of film with the highest thymol content [66]. Furthermore, Lukic et. al., reported that the antioxidant activity of PLA-PLGA films was higher when CT mixture was used, comparing to films containing only carvacrol or thymol [24].

3.3.2. $ABTS^{\bullet+}$ antioxidant assay

The antioxidant activities of tested films were evaluated using $ABTS^{\bullet+}$ free radical method (Figure 3) as well. The benefit of this free radical process is that the reaction between $ABTS^{\bullet+}$ and potassium persulfate is stoichiometric and produced color remains stable for more than 2 days when stored in the dark at room temperature [67].

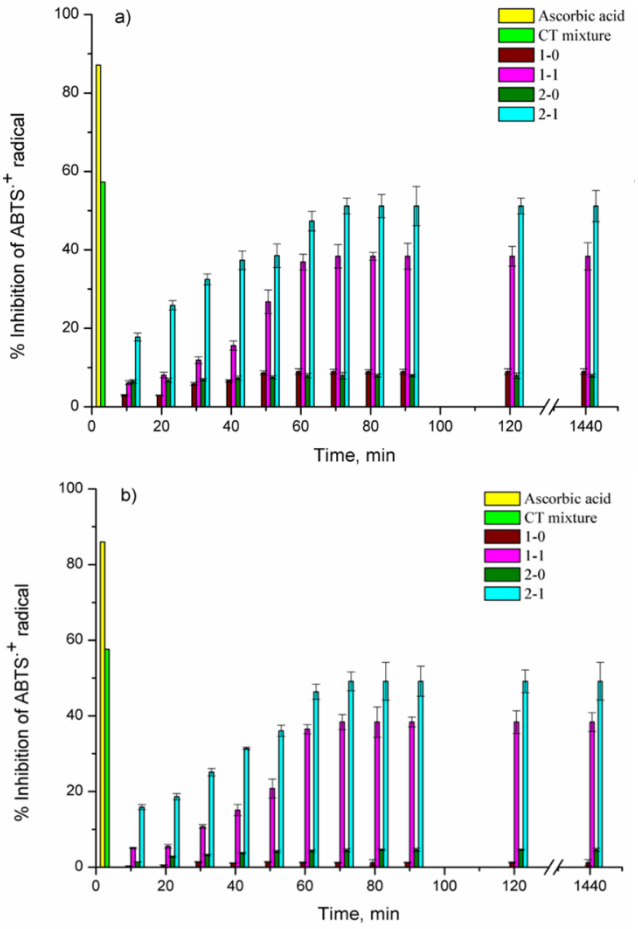

Fig. 3 Antioxidant activity of tested films: a) in water and b) in PBS measured by $ABTS^{\bullet+}$ radical cation expressed as a percent of inhibition

The results obtained by $ABTS^{\bullet+}$ test showed similar trend and somewhat higher activity of tested films with respect to ones obtained for $DPPH^{\bullet}$ analysis in both medium. The water solution of control films showed activities of 9.0 and 7.9%, while PBS solution expressed activities of 1.2 and 4.6% of inhibition for 1-0 and 2-0 samples, respectively (Fig. 3). TC impregnated samples revealed moderate interactions with the ABTS radical cation in comparison to ascorbic acid. The maximum antioxidant activity was observed in the case of 2-1 film, which displayed 51% of inhibition after 1 h and did not change after 2 h and 24 h.

3.4. Release study

Acute wounds heal in an orderly and efficient manner, and progress smoothly through the four different, overlapping stages of healing: haemostasis, inflammation, proliferation and remodeling [68]. Wound dressing materials can accelerate the duration of these phases. In order to exhibit antimicrobial and antioxidant activity, it is necessary that impregnated materials release loaded bioactive components. In addition, for material to be used as wound dressing, the release of loaded bioactive compounds should be in a gradual manner. Some of the parameters that determine release of loaded active compound are type of release medium, as well as morphology and chemistry of polymeric carrier [17]. Therefore, besides buffer solution (pH 7.4) at 37 °C that simulated body fluids, distilled water was also used as model medium for testing of TC release from the impregnated samples to evaluate their possible application as wound dressing material.

3.4.1. *Kinetics of TC mixture release from the impregnated films*

Kinetics of TC mixture release from the impregnated films is presented in Figure 4. It can be seen that both impregnated samples (1-1 and 2-1) expressed initial burst release during first 6 h of the test, whereby the amounts of released TC mixture were around 8 and 37 mg_{TC}/g_{film} in water and 22 and 44 mg_{TC}/g_{film} in PBS medium, respectively. After this period, films exhibited significantly slower release of TC mixture in a gradual manner during tested period of 10 days. The initial burst release is highly desirable to enable delivery of sufficient amount of bioactive compound to the target site at the beginning of the healing process, since it reduces the risk of infections occurrence greatly [69]. Further, sustained release, that enables maintaining of an amount of bioactive compound at target site, is desirable for a prolonged period of time [25]. After 10 days of release experiment, amounts of TC mixture leached from the 2-1 and 1-1 samples were 72% and 29% in the water and 96% and 48% in the PBS media, respectively. Obviously, the higher the loading the higher the release rate was. Similarly, Milovanovic et al. [17] determined that thymol desorption from the impregnated cellulose acetate beads was correlated with the amount of loaded thymol. Thymol release lasted between 2 days (4.5% of loaded thymol) and 21 days (63.0%).

It can be also noticed that the amount of TC mixture was higher in the PBS medium than in the water for both tested films. This observation can be explained by the poor solubility of thymol and carvacrol in water [70], as well as the fact that slightly alkaline media accelerate polymer degradation and promote leaching of loaded substance [71]. A similar effect of chemical nature of the medium on the release rate has been reported for thymol release from cellulose acetate [51] and PLGA [72] used as a carriers. Recently, Lukic et al. reported synergetic

effect of TC mixture, which slow down the release from the PLA films compared to the desorption of single thymol/carvacrol [24]. The amount of released TC mixture in distilled water after 10 days was around 60 mg_{TC}/g_{film} [24]. Similarly, CGZ (2-1) film released around 55 mg_{TC}/g_{film} after 10 days in PBS at 37 °C.

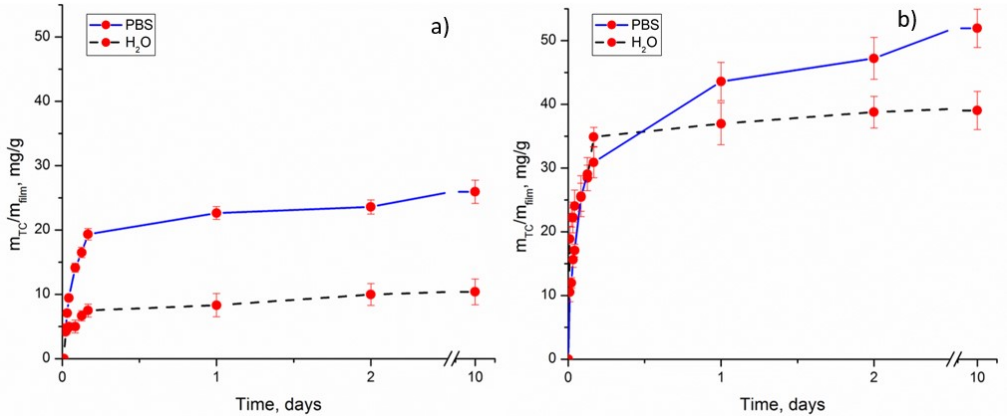

Fig. 4 Kinetic of TC mixture release from impregnated 1-1 and 2-1 films in distilled water (25 °C) and PBS medium (37 °C)

3.4.2. Modeling

The experimental data of release kinetic were correlated with two most frequently used kinetic models (Eqs. 2,3) in order to describe the release mechanism of bioactive components from prepared films. Thus, Weibull function and Higuchi model [73] were applied to simulate the release kinetics of TC mixture from 1-1 and 2-1 films into distilled water and PBS. Determined values of the models parameters are presented in Table 1 and simulation curves at Fig. 5.

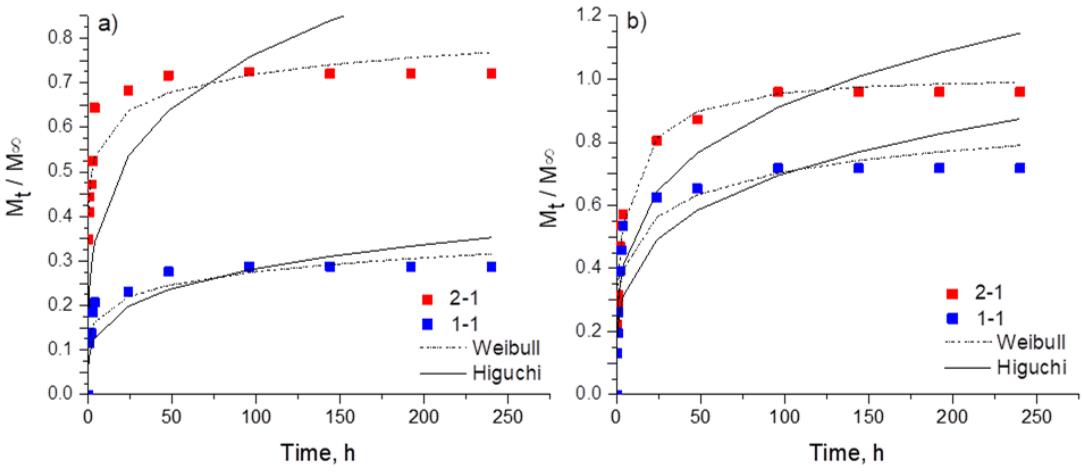

Fig. 5 Relative mass of TC mixture released from the 1-1 and 2-1 films in a) distilled water at 25 °C, b) PBS at 37 °C

Table 1 Parameters and correlation coefficients (R^2) for literature models used for description of TC mixture release kinetics

Film	Release media	Weibull			Higuchi	
		a	*b*	R^2	k_H, $h^{-1/2}$	R^2
2-1	H_2O	0.612	0.159	0.959	0.242	0.217
1-1		0.138	0.185	0.884	0.089	0.766
2-1	PBS	0.420	0.436	0.993	0.222	0.818
1-1		0.346	0.275	0.922	0.291	0.885

The release of active compounds from polymeric matrix through diffusion mechanisms has been already reported for pure thymol and carvacrol release from different materials [51,74,75], as well as for the release of TC mixture from PLA/PCL film into distilled water [24]. When the compound release follows purely Fickian diffusion, a simple and flexible Weibull model is recommended for the entire release profile [74]. Accordingly, the good agreement between experimental values and model was obtained when Weibull model was applied to describe the kinetics of TC mixture release from 1-0 and 2-0 films. Higuchi model gave a significantly lower agreement with the experimental data for all films, with $0.22 < R^2 < 0.89$.

3.5. Characterization of the films

3.5.1. FTIR analysis

To investigate the structural properties of neat and impregnated films and potential interactions between films and TC, FTIR analysis was performed (Figure 6). A set of chitosan characteristic saccharide bands is situated in the range of 1180–900 cm^{-1}. Bands at around 1630, 1516−1538, and 1233−1378 cm^{-1} correspond to the carbonyl group and N-H vibrations in amide I, the amino group and bending vibration of N-H groups in amide II, and C-N stretching and N-H deformation vibrations in amide III respectively, for both gelatine and chitosan [76–78]. Gelatin and chitosan are capable of interactions by formation hydrogen bonds within and between polymer chains involving their carbonyl, hydroxyl and amino groups. This interaction is indicated by the band located at 3270 cm^{-1}, which is shifted to lower wavenumber compared to pure components, as well as a shift in the vibrational wavelengths of the amide I, II and III and saccharide region, between

wavenumbers 1700 and 900 cm^{-1} [76,77]. Absence of unique carboxylic band at about 1690 cm^{-1} might suggest participation of $–COO^-$ groups of gelatin in the electrostatic interaction with positively charged amino groups of chitosan, confirmed by the shift of amide II band of chitosan to higher wavenumber [77]. Electrostatic interactions were also evidenced by the band at 1377 $cm^{-1}$of chitosan recognized as a shoulder of the band at 1410 cm^{-1} in the spectra gelatin [77].

After addition of zeolite to 1-0 films, the apparent decrease in the band intensities at 3270 cm^{-1} as well as the amide I (1632 cm^{-1}) and II (1547 cm^{-1}) was observed, which could be explained as a result of physical inclusion of zeolite in the blends [79]. The bands associated to the presence of zeolite in the film (Si–O–Si, Si–O, and Al–O groups) can be seen in the region of 950–1100 cm^{-1} and are overlapped with the C–O stretching vibrations of 1-0 film, which is visible by broadening of this region band in FTIR spectra (Fig. 6b).

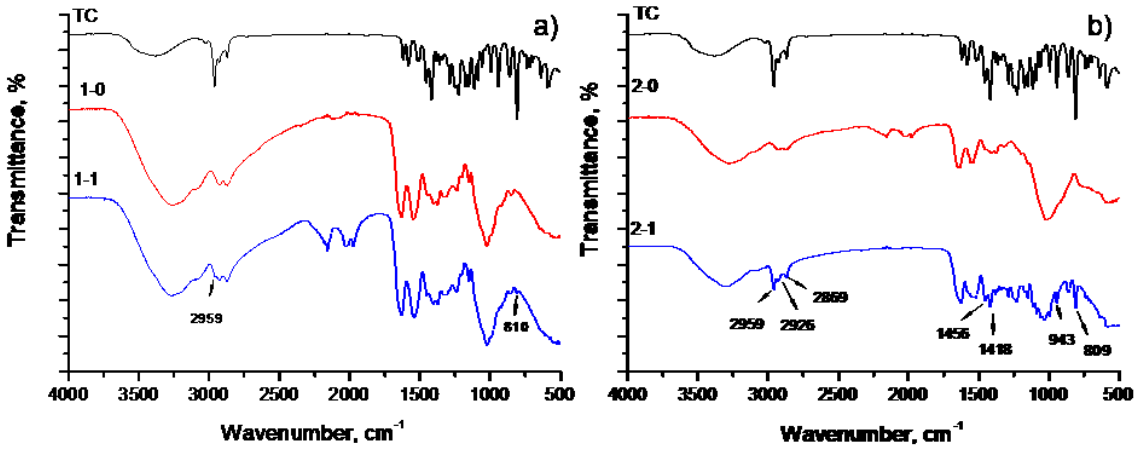

Fig. 6 FTIR spectra of TC mixture, gelatin chitosan and gelatin chitosan zeolite films before and after the SSI

FTIR spectra of TC mixture, recorded for better interpretation of impregnated films spectra, showed characteristic bands of thymol and carvacrol, isomers with similar spectra and differences only in the fingerprint region [22,76]. Presence of TC mixture on the surface of 1-1 film with only 3.3% of TC mixture loading was confirmed by band attributed to the out-of-plane CH wagging vibrations from isoprenoids, appeared at 809 cm^{-1}, arising from the overlapping of thymol and carvacrol bands [24,80]. In addition, band at 2959 cm^{-1} assigned to stretching vibration of CH_3 group originated from TC mixture appeared in the FTIR spectra of 1-1 film (Fig. 6a). Incorporation of TC mixture into the 2-0 film and interactions of phenolic compounds with the polymer matrix through formation of intermolecular hydrogen bonds are more obvious. Aforementioned bands, at 2959 and

809 cm^{-1}, are more intense in the spectra of 2-1 film due to higher amount of TC mixture present in film (Fig. 6b). Beside, shift of the broad band corresponding to stretching vibrations of –OH group to the higher wavenumber (3296 cm^{-1}) compared to neat 2-0 film evidenced the establishing of hydrogen bonds between TC mixture and –OH groups of the 2-0 film [19]. The broadening and lowering intensity of the band at around 1522 cm^{-1}, related to the bending vibration of N–H in amino groups, indicate the participation of these groups in interactions and formation of intermolecular hydrogen bond with –OH groups in phenolic compounds. Furthermore, the bands at 1456, 1418 and 1288 cm^{-1} corresponding to vibrations in phenolic ring of thymol and carvacrol [80]. Bands at around 945 cm^{-1} assigned to =CH out-of-plane bending adsorption [22] are also observed in the FTIR spectra of 2-1 film. Lower intensity of characteristic saccharide bands situated in the range of 1180–900 cm^{-1} and appearance of new bands that correspond to TC mixture also confirmed the incorporation of thymol and carvacrol into the polymer film.

3.5.2. SEM analysis of the films

SEM images of fabricated films before and after the SSI with TC mixture are presented in Fig. 7. Surface and cross section of neat film without zeolite was flat, smooth and homogeneous. Similar images of chitosan gelatin films surface and cross section were already published [19,81]. Addition of zeolite to the chitosan gelatin polymer frame led to the formation of rough structure (Fig. 7c). According to the cross section of 2-0 sample it can be concluded that zeolite particles were fairly distributed through the chitosan gelatin polymer network. The obtained results were in accordance with the study of Milenkovic et al. [82], where the formation of rocky surface of poly(vinyl chloride) films was reported after micronised silver-exchanged natural zeolite (Ag-NZ) was added to the polymer frame.

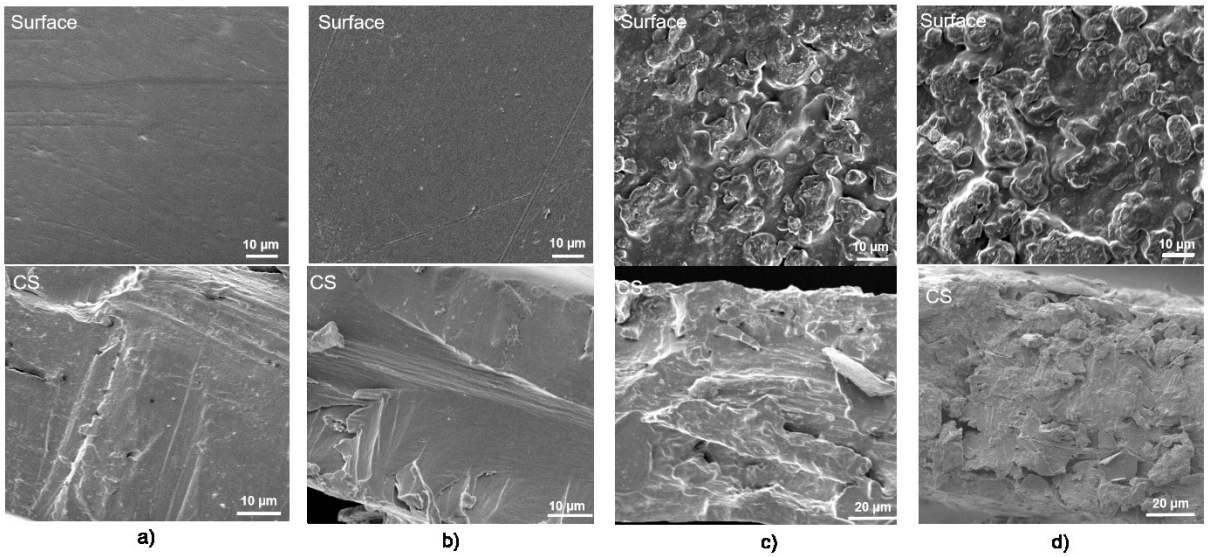

Fig. 7 SEM images of surface and cross section (CS) of a) 1-0, b) 1-1, c) 2-0 and d) 2-1 films

As can be seen, the SSI did not affect the morphology of the prepared films film remarkably (Fig. 7b and 7c). The polymer melting was not observed in the case of 1-1 neither for 2-1 sample, which was in agreement with the results of thermal analysis (Section 3.5.3).

3.5.3. TG-DTG analysis

Thermal analysis of the prepared films showed that in the observed temperature range up to 600 °C, weight loss occurs through three steps in the case of control samples, while TC impregnated films expressed two stage weight loss. Thermal degradation of control 1-0 sample (Fig. 8a) fits well the literature data [19]. DTG curve of control 1-0 film showed three maxima at 70.6, 172.7 and 290.1 °C with corresponding weight losses of 8.1, 13.7 and 47.6%, respectively. Incorporation of zeolite led to the formation of less thermally stable matrix (Fig. 8b) since degradation temperatures were shifted to lower values of 60.6, 162.9 and 284.8 °C, while corresponding weight losses were 9.4, 11.2 and 40.3%, respectively. First degradation step corresponds to the molecules of the adsorbed water, while weight losses in the temperature range of 110-500 °C are related to the decomposition of gelatin and chitosan for both 1-0 and 2-0 samples.

The SSI of films with TC mixture enabled formation of films with improved thermal properties. Indeed, degradation temperatures were shifted to somewhat higher values (Fig. 7). Increased thermal stability of the films loaded with TC mixture can be explained by formation of hydrogen bonds between thymol/carvacrol and polymer network, which was confirmed by FTIR analysis. Accordingly, DTG curves of the impregnated samples did not displayed maxima characteristics for pure thymol (160 °C) [83] nor for pure carvacrol (170 °C) [84] related to decomposition of these compounds.

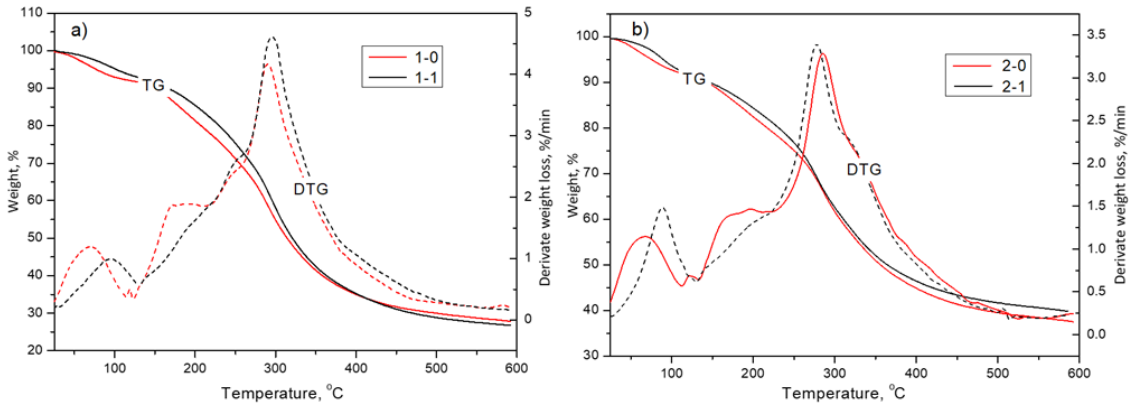

Fig. 8 TGA-DTG analysis of control and TC loaded films a) 1-0 and b) 2-0

3.5.4. Barrier properties of the films

The results of WVP analysis are shown in Table 2. It can be seen that the permeability values of pure 1-0 films were lower compared to the 2-0 samples due to the presence of zeolite. Namely, it can be assumed that increased gaps between polymer chains inside the matrix of the 2-0 film contributed to formation of the polymer network that become less dense and more open to the adsorption/desorption of water molecules [32]. The obtained values of WVP of the films were in agreement with the literature. WVP of gelatin/chitosan films was $1.83 \cdot 10^{-10}$ $gm^{-1}s^{-1}Pa^{-1}$ [85], while gelatin/ carboxymethyl cellulose/chitosan composite exhibited WVP in the range from $1.21 \cdot 10^{-8}$ to $6.13 \cdot 10^{-10}$ $gm^{-1}s^{-1}Pa^{-1}$ [86]. Similarly, bi-layer CG films showed WVP of 1.11 and $1.20 \cdot 10^{-10}$ $gm^{-1}s^{-1}Pa^{-1}$ [87].

Loading of TC mixture decreased the WVP of both films compared to neat films. This observation is in accordance with the previously reported results where WVP of the polymer films decreased after the addition of hydrophobic compound [32]. The lowest WVP was observed in the case of the 1-1 film ($8.2 \cdot 10^{-11}$ $gm^{-1}s^{-1}Pa^{-1}$).

According to the values of WVTR (Table 2) fabricated films could be considered promising candidates for wound healing application as literature reports WVTR in the range of 76–9360 g/m^2 day, appropriate for materials suitable for this purpose [39].

Table 2 Water vapor transmission rate (WVTR) and WVP of the control and TC impregnated films.

	1-0	**1-1**	**2-0**	**2-1**
$D_{average}$, mm	0.147±0.01	0.145±0.01	0.165±0.01	0.160±0.01
WVTR, gm^{-2} day^{-1}	143.3±11.3	115.4±10.8	161.1±17.8	127.1±10.9
WVP $\cdot 10^{11}$, $gm^{-1}s^{-1}Pa^{-1}$	10.4±0.71	8.2±0.62	13.0±1.1	10.3±0.89

$D_{average}$-average thickness of the films

3.5.5. Solubility of films

Results of solubility test in water are summarized in Table 3.

Table 3 Solubility of fabricated films in water

Solubility values of tested films were above 30% indicating high degree of gelatin and chitosan cross-linking [43]. Namely, gelatin as water soluble compound can easily lose its fibrous structure in high ambient humidity conditions. However, mixing gelatin with other functional materials, such as chitosan, can induce crosslinking and stabilization of gelatin structure and consequently decrease its solubility in aqueous medium [88]. As expected, presence of zeolite led to the higher solubility of fabricated materials (2-0). The increase in percentage of solubility of around 30% could be induced by physical incorporation of zeolite particles into the film and obstruction of the polymer chains of chitosan and gelatin. This is supported by the reduced value of cross-linking in the case of 2-0 sample compared to the cross-linking degree of film without zeolite. After the SSI solubility of films increased in both tested materials (1-1 and 2-1). Obtained results are in accordance with the literature, since it was already published that solubility of gelatin-chitosan films significantly increased in the presence of essential oil [89]. Furthermore, Kavoosi et al. [43] reported that incorporation of thymol caused an increase in solubility of gelatin films. The amount of thymol added to the gelatin films was in the range of 1-8% and it was noticeable that the higher the thymol amount was the higher the films' solubility was [43]. Similarly, higher solubility was observed in the case of 2-1 sample with higher amount of incorporated bioactive compounds compared to the solubility of 1-1 film. It can be assumed that TC molecules interfere the polymer chain-to-chain interactions and lead to the slight decrease in degree of chitosan-gelatin cross-linking. However, according to results from Table 2 it can be concluded that even after incorporation of TC mixture into the films the increase in solubility was not significant and the films retained cross-linking structure.

	1-0	**1-1**	**2-0**	**2-1**
Solubility in water, %	10.2±2.3	18.0±4.1	14.6 ±1.9	22.2 0 ±2.2
Cross-linking, %	89.8±12.2	82.0±5.8	79.1±7.7	68.4±5.7

3.5.6. Swelling test of films

An important characteristic for wound dressing materials is their ability to swell, in order to enable conditions for moist wound healing [90]. Morgado et al. reported that an ideal wound dressing film should have ability for water uptake between 100-900% [91].

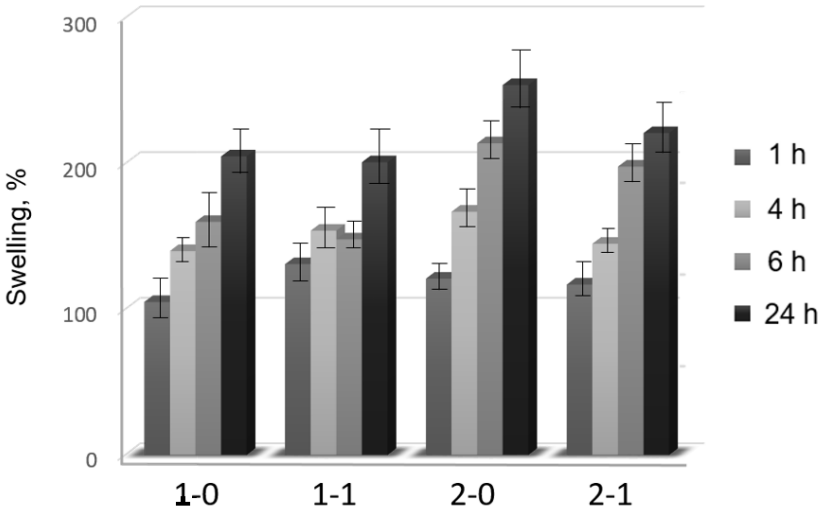

Fig. 9 Swelling ratio of the films

Tested materials showed moderate swelling degree (Fig. 9), indicating preservation of structural integrity for tested period of time. Slightly higher swelling values were observed for films containing zeolite. As previously mentioned, it could be assumed that incorporation of zeolite into the material hinder the chitosan gelatin polymer network. In addition, presence of alkaline media might have induced formation of gaps between polymer network and enable easer diffusion of buffer molecules into the material. Presence of TC mixture induced lowering of swelling capacity of films, probably due to its hydrophobic nature. Similarly, decrease in material swelling after incorporation of thymol was previously reported [43].

3.5.7. Mechanical analysis

Mechanical properties of both neat and impregnated films, namely, tensile strength (σ) as a measure of maximum stress that material can withstand before breaking, Young's modulus (E) which quantifies film flexibility, and elongation at break (ε) which quantifies the capacity of film to extend before breaking, are shown in Table 4.

Table 4 Mechanical properties of neat and impregnated films

Film	**σ, MPa**	**E, MPa**	**ε, %**
1-0	0.70±0.08	103.90±13.46	1.55±0.13
2-0	0.51±0.04	85.68±8.84	1.60±0.12

1-1	0.48±0.05	108.70±11.53	0.82±0.04
2-1	0.40±0.03	67.18±7.01	1.36±0.08

As can be seen, addition of zeolite to 1-0 films decreased σ and E, while ε remains almost unchanged. A reduction in mechanical strength when added amount of zeolite is higher than 20% is explained by the formation of too many interfacial voids at the interface of chitosan and zeolite [92]. The same observation was previously reported for starch/chitosan films that contained different amounts of zeolite [32]. Decreased values of Young's modulus after impregnation of TC mixture into 2-0 film revealed that more flexible film was obtained by loading of active substances due to their possible plasticizing effect [24], while elongation at break only slightly changed from 1.60 to 1.36%. Values of tensile strength of the obtained films were up to 0.7 MPa. Similarly, values ranging between 0.58-1.38 MPa were reported for scaffolds prepared from solutions of various chitosan concentrations [93], as well as for chitosan/gelatin films (1.74 MPa) [94].

Loading of TC mixture into the 1-0 and 2-0 films caused decrease of the values of σ by 32 and 20%, respectively, compared to non-impregnated films. Although opposite could be found in the literature [60], our results are in accordance with many studies, where the addition of active compounds has been reported to reduce the σ of polymer films. After adding of *Origanum vulgare* and orange peel essential oil to fish gelatin/chitosan film, σ decline of 36–69% and 9–21%, respectively, was reported [95,96], while loading of TC mixture into PLA/PCL film reduced the value of σ by 78% [24]. It was proposed that essential oils affect the microstructure of polymer matrix by rearrangement of polymeric chains. The interactions between chitosan and gelatin molecules are partially replaced by the weaker polymer-oil interaction in the film matrix [40,97].

CONCLUSION

Proposed SSI technique was successfully applied for loading of TC mixture into the prepared chitosan/gelatin (CG) and chitosan/gelatin/zeolite films (CGZ) for the first time. Addition of zeolite to CG blend enhanced films' loading capacity enabling higher amount (6.0%) of incorporated TC mixture in comparison to the CG film. FTIR analysis confirmed presence of thymol/carvacrol on the surface of the impregnated films as well as formation of hydrogen bonds between thymol/carvacrol and chitosan/gelatin. Loading of TC mixture slightly decreased WVP and increased thermal stability of developed films compared to the control samples. Barrier properties prepared films were in the range of those materials suitable for wound dressing

purposes. Results of the release study in both water and PBS (pH 7.4) media revealed initial burst release during the first 6 h of the test, followed by the gradual release profile during next 10 days. Amounts of TC mixture released from the CG and CGZ films in PBS medium were around 22 and 44 mg TC/g film, respectively. Weibull model was found to be the most appropriate model for the release data correlation. Both antibacterial and antioxidant activity of the CG and CGZ films impregnated with TC mixture were proven. Tested materials showed low water solubility and moderate swelling properties in PBS (pH 7.4). Results of the present study revealed high potential of fabricated material with biological properties and could be used for further development of wound dressings.

Acknowledgements

This work was supported by the Ministry of Education, Science and Technological Development of the Republic of Serbia (Contract No. 451-03-68/2022-14/200287 and 451-03-68/2022-14/200135). Work was carried out in the frame of the COST-Action "Green Chemical Engineering Network towards upscaling sustainable processes" (GREENERING, ref. CA18224) funded by the European Commission.

The authors would like to thank dr Stevan Stupar for performing SEM analysis.

Conflict of interest or competing interests:

Authors declare that no conflicts of interest exist.

Data availability

The raw/processed data required to reproduce these findings cannot be shared at this time due to legal or ethical reasons.

Literature

[1] Mazid M, Khan TA, Mohammad F. Role of secondary metabolites in defense mechanisms of plants. Biology and Medicine 2011;3:232–49.

[2] Magi G, Marini E, Facinelli B. Antimicrobial activity of essential oils and carvacrol, and synergy of carvacrol and erythromycin, against clinical, erythromycin-resistant Group A Streptococci. Frontiers in Microbiology 2015;6:1–7. https://doi.org/10.3389/fmicb.2015.00165.

[3] Bouarab Chibane L, Degraeve P, Ferhout H, Bouajila J, Oulahal N. Plant antimicrobial polyphenols as potential natural food preservatives. Journal of the Science of Food and Agriculture 2019;99:1457–74. https://doi.org/10.1002/jsfa.9357.

[4] Nitiema LW, Savadogo A, Simpore J, Dianou D, Traore AS. In vitro antimicrobial activity of some phenolic compounds (coumarin and quercetin) against gastroenteritis bacterial strains. International Journal of Microbiological Research 2012;3:183–7. https://doi.org/10.5829/idosi.ijmr.2012.3.3.6414.

[5] Antonia Nostro, Teresa Papalia. Antimicrobial Activity of Carvacrol: Current Progress and Future Prospectives. Recent Patents on Anti-Infective Drug Discovery 2012;7:28–35. https://doi.org/10.2174/157489112799829684.

[6] Nagoor Meeran MF, Javed H, Taee H Al, Azimullah S, Ojha SK. Pharmacological properties and molecular mechanisms of thymol: Prospects for its therapeutic potential and pharmaceutical development. Frontiers in Pharmacology 2017;8:1–34. https://doi.org/10.3389/fphar.2017.00380.

[7] Nostro A, Blanco AR, Cannatelli MA, Enea V, Flamini G, Morelli I, et al. Susceptibility of methicillin-resistant staphylococci to oregano essential oil, carvacrol and thymol. FEMS Microbiology Letters 2004;230:191–5. https://doi.org/10.1016/S0378-1097(03)00890-5.

[8] Campos-Requena VH, Rivas BL, Perez MA, Figueroa CR, Sanfuentes EA. The synergistic antimicrobial effect of carvacrol and thymol in clay/polymer nanocomposite films over strawberry gray mold. LWT - Food Science and Technology 2015;64:390–6. https://doi.org/10.1016/j.lwt.2015.06.006.

[9] Krepker M, Shemesh R, Danin Poleg Y, Kashi Y, Vaxman A, Segal E. Active food packaging films with synergistic antimicrobial activity. Food Control 2017;76:117–26. https://doi.org/10.1016/j.foodcont.2017.01.014.

[10] Rivas L, McDonnell MJ, Burgess CM, O'Brien M, Navarro-Villa A, Fanning S, et al. Inhibition of verocytotoxigenic Escherichia coli in model broth and rumen systems by carvacrol and

thymol. International Journal of Food Microbiology 2010;139:70–8. https://doi.org/10.1016/j.ijfoodmicro.2010.01.029.

[11] Braga MEM, Pato MTV, Silva HSRC, Ferreira EI, Gil MH, Duarte CMM, et al. Supercritical solvent impregnation of ophthalmic drugs on chitosan derivatives. Journal of Supercritical Fluids 2008;44:245–57. https://doi.org/10.1016/j.supflu.2007.10.002.

[12] Dias AM., Braga ME., Seabra IJ, Ferreira P, Gil M., De Sousa H. Development of natural-based wound dressings impregnated with bioactive compounds and using supercritical carbon dioxide. International Journal of Pharmaceutics 2011;408:9–19. https://doi.org/10.1016/j.ijpharm.2011.01.063.

[13] Zizovic I, Ivanovic J, Milovanovic S, Stamenic M. Impregnations using supercritical carbon dioxide. In: Rój E, editor. Supercritical CO2 extraction and its applications, Lublin, Poland: OIC Poland; 2014, p. 23–34.

[14] Milovanovic S, Jankovic-Castvan I, Ivanovic J, Zizovic I. Effect of starch xero- And aerogels preparation on the supercritical CO2 impregnation of thymol. Starch/Staerke 2015;67:174–82. https://doi.org/10.1002/star.201400134.

[15] Boyère C, Jérôme C, Debuigne A. Input of supercritical carbon dioxide to polymer synthesis: An overview. European Polymer Journal 2014;61:45–63. https://doi.org/10.1016/j.eurpolymj.2014.07.019.

[16] Monteagudo-Olivan R, Cocero MJ, Coronas J, Rodríguez-Rojo S. Supercritical CO 2 encapsulation of bioactive molecules in carboxylate based MOFs. Journal of CO2 Utilization 2019;30:38–47. https://doi.org/10.1016/j.jcou.2018.12.022.

[17] Milovanovic S, Stamenic M, Markovic D, Ivanovic J, Zizovic I. Supercritical impregnation of cellulose acetate with thymol. Journal of Supercritical Fluids 2015;97:107–15. https://doi.org/10.1016/j.supflu.2014.11.011.

[18] Pajnik J, Radetić M, Stojanovic DB, Jankovic-Častvan I, Tadic V, Stanković M V., et al. Functionalization of polypropylene, polyamide and cellulose acetate materials with pyrethrum extract as a natural repellent in supercritical carbon dioxide. Journal of Supercritical Fluids 2018;136:70–81. https://doi.org/10.1016/j.supflu.2018.02.014.

[19] Radovic M, Adamovic T, Pavlovic J, Rusmirovic J, Tadic V, Brankovic Z, et al. Supercritical CO2 impregnation of gelatin-chitosan films with clove essential oil and characterization thereof. Chemical Industry and Chemical Engineering Quarterly 2019;25:119–30.

https://doi.org/10.2298/CICEQ180323025R.

[20] Torres A, Ilabaca E, Rojas A, Rodríguez F, Galotto MJ, Guarda A, et al. Effect of processing conditions on the physical, chemical and transport properties of polylactic acid films containing thymol incorporated by supercritical impregnation. European Polymer Journal 2017;89:195–210. https://doi.org/10.1016/j.eurpolymj.2017.01.019.

[21] Milovanovic S, Markovic D, Mrakovic A, Kuska R, Zizovic I. Materials Science & Engineering C Supercritical CO 2 - assisted production of PLA and PLGA foams for controlled thymol release. Materials Science & Engineering C 2019;99:394–404. https://doi.org/10.1016/j.msec.2019.01.106.

[22] Milovanovic S, Hollermann G, Errenst C, Pajnik J, Frerich S, Kroll S, et al. Supercritical CO2 impregnation of PLA/PCL films with natural substances for bacterial growth control in food packaging. Food Research International 2018;107:486–95. https://doi.org/https://doi.org/10.1016/j.foodres.2018.02.065.

[23] Rojas A, Torres A, Martínez F, Salazar L, Villegas C, Galotto MJ, et al. Assessment of kinetic release of thymol from LDPE nanocomposites obtained by supercritical impregnation: Effect of depressurization rate and nanoclay content. European Polymer Journal 2017;93:294–306. https://doi.org/10.1016/j.eurpolymj.2017.05.049.

[24] Lukic I, Vulic J, Ivanovic J. Antioxidant activity of PLA/PCL films loaded with thymol and/or carvacrol using scCO2 for active food packaging. Food Packaging and Shelf Life 2020;26:100578. https://doi.org/10.1016/j.fpsl.2020.100578.

[25] Patel S, Srivastava S, Singh MR, Singh D. Preparation and optimization of chitosan-gelatin films for sustained delivery of lupeol for wound healing. International Journal of Biological Macromolecules 2018;107:1888–97. https://doi.org/10.1016/j.ijbiomac.2017.10.056.

[26] Matica MA, Aachmann FL, Tøndervik A, Sletta H, Ostafe V. Chitosan as a wound dressing starting material: Antimicrobial properties and mode of action. International Journal of Molecular Sciences 2019;20:1–33. https://doi.org/10.3390/ijms20235889.

[27] Subramanian K, Indumathi S, Vijayakumar V. Fabrication and Evaluation of Chitosan-Gelatin Composite Film As a Drug Carrier for in Vitro Transdermal Delivery. International Journal of Pharmaceutical Sciences and Research 2014;5:438. https://doi.org/10.13040/IJPSR.0975-8232.5(2).438-47.

[28] Farías T, de Ménorval LC, Zajac J, Rivera A. Solubilization of drugs by cationic surfactants

micelles: Conductivity and1H NMR experiments. Colloids and Surfaces A: Physicochemical and Engineering Aspects 2009;345:51–7. https://doi.org/10.1016/j.colsurfa.2009.04.022.

[29] Hayakawa K, Mouri Y, Maeda T, Satake I, Sato M. Surfactant-modified zeolites as a drug carrier and the release of chloroquin. Colloid and Polymer Science 2000;278:553–8. https://doi.org/10.1007/s003960050554.

[30] Li Z, Bowman RS. Sorption of perchloroethylene by surfactant-modified zeolite as controlled by surfactant loading. Environmental Science and Technology 1998;32:2278–82. https://doi.org/10.1021/es971118r.

[31] Kaya DA, Vuluga Z, Nicolae CA, Radovici C, Albu MG. The properties of two natural zeolites modified with oregano essential oil. Romanian Journal of Materials 2013;43:48–54.

[32] Pajnik J, Lukić I, Dikic J, Asanin J, Gordic M, Misic D, et al. Application of Supercritical Solvent Impregnation for Production of Zeolite Modified Starch-Chitosan Polymers with Antibacterial Properties. Molecules 2020;25:4717–35. https://doi.org/10.3390/molecules25204717.

[33] Garcia-Basabe Y, Rodriguez-Iznaga I, De Menorval LC, Llewellyn P, Maurin G, Lewis DW, et al. Step-wise dealumination of natural clinoptilolite: Structural and physicochemical characterization. Microporous and Mesoporous Materials 2010;135:187–96. https://doi.org/10.1016/j.micromeso.2010.07.008.

[34] Pajnik J, Stamenić M, Radetić M, Tomanović S, Sukara R, Mihaljica D, et al. Impregnation of cotton fabric with pyrethrum extract in supercritical carbon dioxide. The Journal of Supercritical Fluids 2017;128:66–72. https://doi.org/10.1016/j.supflu.2017.05.006.

[35] Ramos M, Beltrán A, Peltzer M, Valente AJM, Garrigós C. LWT - Food Science and Technology Release and antioxidant activity of carvacrol and thymol from polypropylene active packaging fi lms. LWT - Food Science and Technology 2014;58:470–7. https://doi.org/10.1016/j.lwt.2014.04.019.

[36] López-mata MA, Ruiz-cruz S, Silva-beltrán NP, Ornelas-paz JDJ, Ocaño-higuera VM, Rodríguez-félix F, et al. Physicochemical and Antioxidant Properties of Chitosan Films Incorporated with Cinnamon Oil. International Journal of Polymer Science 2015;2015:974506.

[37] Ren L, Yan X, Zhou J, Tong J, Su X. Influence of chitosan concentration on mechanical and barrier properties of corn starch/chitosan films. International Journal of Biological Macromolecules 2017;105:1636–43. https://doi.org/10.1016/j.ijbiomac.2017.02.008.

[38] Hosseini MH, Razavi SH, Mousavi MA. Antimicrobial, physical and mechanical properties of

chitosan-based films incorporated with thyme, clove and cinnamon essential oils. Journal of Food Processing and Preservation 2009;33:727–43. https://doi.org/10.1111/j.1745-4549.2008.00307.x.

[39] Wu P, Fisher AC, Foo PP, Queen D, Gaylor JDS. In vitro assessment of water vapour transmission of synthetic wound dressings. Biomaterials 1995;16:171–5. https://doi.org/10.1016/0142-9612(95)92114-L.

[40] Haghighi H, Biard S, Bigi F, Leo R De, Bedin E, Pfeifer F, et al. Comprehensive characterization of active chitosan-gelatin blend fi lms enriched with di fferent essential oils. Food Hydrocolloids 2019;95:33–42. https://doi.org/10.1016/j.foodhyd.2019.04.019.

[41] Ahmad M, Benjakul S, Prodpran T, Agustini TW. Physico-mechanical and antimicrobial properties of gelatin film from the skin of unicorn leatherjacket incorporated with essential oils. Food Hydrocolloids 2012;28:189–99. https://doi.org/10.1016/j.foodhyd.2011.12.003.

[42] Núñez-Flores R, Giménez B, Fernández-Martín F, López-Caballero ME, Montero MP, Gómez-Guillén MC. Physical and functional characterization of active fish gelatin films incorporated with lignin. Food Hydrocolloids 2013;30:163–72. https://doi.org/10.1016/j.foodhyd.2012.05.017.

[43] Kavoosi G, Dadfar SMM, Purfard AM. Mechanical, Physical, Antioxidant, and Antimicrobial Properties of Gelatin Films Incorporated with Thymol for Potential Use as Nano Wound Dressing. Journal of Food Science 2013;78:E224–50. https://doi.org/10.1111/1750-3841.12015.

[44] Ahmad A, Khan A, Akhtar F, Yousuf S, Xess I, Khan LA, et al. Fungicidal activity of thymol and carvacrol by disrupting ergosterol biosynthesis and membrane integrity against Candida. European Journal of Clinical Microbiology and Infectious Diseases 2011;30:41–50. https://doi.org/10.1007/s10096-010-1050-8.

[45] Champeau M, Thomassin JM, Tassaing T, Jérôme C. Drug loading of polymer implants by supercritical CO2 assisted impregnation: A review. Journal of Controlled Release 2015;209:248–59. https://doi.org/10.1016/j.jconrel.2015.05.002.

[46] Goñi ML, Gañán NA, Strumia MC, Martini RE. Eugenol-loaded LLDPE films with antioxidant activity by supercritical carbon dioxide impregnation. Journal of Supercritical Fluids 2016;111:28–35. https://doi.org/10.1016/j.supflu.2016.01.012.

[47] Dikić J, Lukić I, Pajnik J, Pavlović J, Hrenović J, Rajić N. Antibacterial activity of

thymol/carvacrol and clinoptilolite composites prepared by supercritical solvent impregnation. Journal of Porous Materials 2021. https://doi.org/10.1007/s10934-021-01107-y.

[48] Gómez-Estaca J, López de Lacey A, López-Caballero ME, Gómez-Guillén MC, Montero P. Biodegradable gelatin e chitosan fi lms incorporated with essential oils as antimicrobial agents for fi sh preservation. Food Microbiology 2010;27:889–96. https://doi.org/10.1016/j.fm.2010.05.012.

[49] Milenkovic J, Hrenovic J, Matijasevic D, Niksic M, Rajic N. Bactericidal activity of Cu-, Zn-, and Ag-containing zeolites toward Escherichia coli isolates. Environmental Science and Pollution Research 2017;24:20273–81. https://doi.org/10.1007/s11356-017-9643-8.

[50] Hrenovic J, Milenkovic J, Ivankovic T, Rajic N. Antibacterial activity of heavy metal-loaded natural zeolite. Journal of Hazardous Materials 2012;201–202:260–4. https://doi.org/10.1016/j.jhazmat.2011.11.079.

[51] Milovanovic S, Markovic D, Aksentijevic K, Stojanovic DB, Ivanovic J, Zizovic I. Application of cellulose acetate for controlled release of thymol. Carbohydrate Polymers 2016;147:344–53. https://doi.org/10.1016/j.carbpol.2016.03.093.

[52] Trombetta D, Castelli F, Grazia M, Venuti V, Cristani M, Saija A, et al. Mechanisms of Antibacterial Action of Three Monoterpenes Mechanisms of Antibacterial Action of Three Monoterpenes. Antimicrobial Agents and Chemotherapy 2005;9:2474–8. https://doi.org/10.1128/AAC.49.6.2474.

[53] Burt S. Essential oils: Their antibacterial properties and potential applications in foods - A review. International Journal of Food Microbiology 2004;94:223–53. https://doi.org/10.1016/j.ijfoodmicro.2004.03.022.

[54] Nazzaro F, Fratianni F, De Martino L, Coppola R, De Feo V. Effect of essential oils on pathogenic bacteria. Pharmaceuticals 2013;6:1451–74. https://doi.org/10.3390/ph6121451.

[55] García-Salinas S, Elizondo-Castillo H, Arruebo M, Mendoza G, Irusta S. Evaluation of the antimicrobial activity and cytotoxicity of different components of natural origin present in essential oils. Molecules 2018;23. https://doi.org/10.3390/molecules23061399.

[56] Comino-Sanz IM, López-Franco MD, Castro B, Pancorbo-Hidalgo PL. The role of antioxidants on wound healing: A review of the current evidence. Journal of Clinical Medicine 2021;10. https://doi.org/10.3390/jcm10163558.

[57] Altiok D, Altiok E, Tihminlioglu F. Physical, antibacterial and antioxidant properties of chitosan films incorporated with thyme oil for potential wound healing applications. Journal of Materials Science: Materials in Medicine 2010;21:2227–36. https://doi.org/10.1007/s10856-010-4065-x.

[58] Avelelas F, Horta A, Pinto LFV, Marques SC, Nunes PM, Pedrosa R, et al. Antifungal and antioxidant properties of chitosan polymers obtained from nontraditional Polybius henslowii sources. Marine Drugs 2019;17. https://doi.org/10.3390/md17040239.

[59] Kim KW, Thomas RL. Antioxidative activity of chitosans with varying molecular weights. Food Chemistry 2007;101:308–13. https://doi.org/10.1016/j.foodchem.2006.01.038.

[60] Hosseini SF, Ghaderi J, Gómez-Guillén MC. trans-Cinnamaldehyde-doped quadripartite biopolymeric films: Rheological behavior of film-forming solutions and biofunctional performance of films. Food Hydrocolloids 2021;112. https://doi.org/10.1016/j.foodhyd.2020.106339.

[61] Shahidi F, Ambigaipalan P. Phenolics and polyphenolics in foods , beverages and spices : Antioxidant activity and health effects –. Journal of Functional Foods 2015;18:820–97. https://doi.org/10.1016/j.jff.2015.06.018.

[62] Ichikawa K, Sasada R, Chiba K, Gotoh H. Effect of Side Chain Functional Groups on the DPPH Radical Scavenging Activity of Bisabolane-Type. Antioxidans 2019;65:8030065. https://doi.org/10.3390/antiox8030065.

[63] Leopoldini M, Marino T, Russo N, Toscano M. Antioxidant Properties of Phenolic Compounds : H-Atom versus Electron Transfer Mechanism. J Phys Chem 2004;108:4916–22. https://doi.org/10.1021/jp037247d.

[64] Hussain HH, Babic G, Durst T, Wright JS, Flueraru M, Chichirau A, et al. Development of Novel Antioxidants : Design , Synthesis , and Reactivity. J Org Chem 2003:7023–32.

[65] Kavoosi G, Dadfar SMM, Purfard AM. Mechanical, Physical, Antioxidant, and Antimicrobial Properties of Gelatin Films Incorporated with Thymol for Potential Use as Nano Wound Dressing. Journal of Food Science 2013;78:240–50. https://doi.org/10.1111/1750-3841.12015.

[66] Zhong T, Liang Y, Jiang S, Yang L, Shi Y, Guo S, et al. Physical, antioxidant and antimicrobial properties of modified peanut protein isolate based films incorporating thymol. RSC Advances 2017;7:41610–8. https://doi.org/10.1039/c7ra07444a.

[67] Re R, Pellegrini N, Proteggente A, Pannala A, Yang M, Rice-Evans C. ANTIOXIDANT ACTIVITY APPLYING AN IMPROVED ABTS RADICAL. Free Radical Biology & Medicine 1999;26:1231–7.

[68] Bennett NT, Schultz GS. Growth factors and wound healing: Part II. Role in normal and chronic wound healing. The American Journal of Surgery 1993;166:74–81.

[69] Syukri DM, Nwabor OF, Singh S, Ontong JC. Antibacterial-coated silk surgical sutures by ex situ deposition of silver nanoparticles synthesized with Eucalyptus camaldulensis eradicates infections. Journal of Microbiological Methods 2020;174:105955. https://doi.org/10.1016/j.mimet.2020.105955.

[70] Mastelic J, Jerkovic I, Blazevic I, Poljak-Blazi M, Borovic S, Ivancic-Bace I, et al. Comparative Study on the Antioxidant and Biological Activities of Carvacrol , Thymol , and Eugenol. J Agric Food Chem 2008;56:3989–96.

[71] Holy CE, Dang SM, Davies JE, Shoichet MS. In vitro degradation of a novel poly(lactide-co-glycolide) 75/25 foam. Biomaterials 1999;20:1177–85. https://doi.org/10.1016/S0142-9612(98)00256-7.

[72] Milovanovic S, Markovic D, Mrakovic A, Kuska R, Zizovic I, Frerich S, et al. Supercritical CO 2 -assisted production of PLA and PLGA foams for controlled thymol release. Materials Science and Engineering C 2019;99:394–404. https://doi.org/10.1016/j.msec.2019.01.106.

[73] Higuchi T. Mechanism of sustained-action medication. Theoretical analysis of rate of release of solid drugs dispersed in solid matrices. Journal of Pharmaceutical Sciences 1963;52:1145–9. https://doi.org/10.1002/jps.2600521210.

[74] Ulloa PA, Guarda A, Valenzuela X, Rubilar JF. Modeling the release of antimicrobial agents (thymol and carvacrol) from two different encapsulation materials. Food Science and Biotechnology 2017;26:1763–1772. https://doi.org/10.1007/s10068-017-0226-8.

[75] Keawchaoon L, Yoksan R. Colloids and Surfaces B : Biointerfaces Preparation , characterization and in vitro release study of carvacrol-loaded chitosan nanoparticles. Colloids and Surfaces B: Biointerfaces 2011;84:163–71. https://doi.org/10.1016/j.colsurfb.2010.12.031.

[76] Altan A, Aytac Z, Uyar T. Carvacrol loaded electrospun fibrous films from zein and poly(lactic acid) for active food packaging. Food Hydrocolloids 2018;81:48–59. https://doi.org/10.1016/j.foodhyd.2018.02.028.

[77] Staroszczyk H, Sztuka K, Wolska J, Wojtasz-paja A. Interactions of fish gelatin and chitosan in

uncrosslinked and crosslinked with EDC films : FT-IR study. Spectrochimica Acta Part A : Molecular and Biomolecular Spectroscopy 2014;117:707–12. https://doi.org/10.1016/j.saa.2013.09.044.

[78] Jridi M, Hajji S, Ben H, Lassoued I, Mbarek A, Kammoun M, et al. Physical , structural , antioxidant and antimicrobial properties of gelatin – chitosan composite edible films. International Journal of Biological Macromolecules 2014;67:373–9. https://doi.org/10.1016/j.ijbiomac.2014.03.054.

[79] Giménez B, Montero P. Role of sepiolite in the release of active compounds from gelatin e egg white fi lms. Food Hydrocolloids 2012;27:475–86. https://doi.org/10.1016/j.foodhyd.2011.09.003.

[80] Topala CM, Tataru LD. ATR-FTIR Study of Thyme and Rosemary Oils Extracted by Supercritical Carbon Dioxide. Revista de Chimie 2016;67:842–846.

[81] Sakthiguru N, Sithique MA. Fabrication of bioinspired chitosan/gelatin/allantoin biocomposite film for wound dressing application. International Journal of Biological Macromolecules 2020;152:873–83. https://doi.org/10.1016/j.ijbiomac.2020.02.289.

[82] Milenkovic J, Hrenovic J, Goic-Barisic I, Tomic M, Djonlagic J, Rajic N. Synergistic anti-biofouling effect of Ag-exchanged zeolite and D-Tyrosine on PVC composite against the clinical isolate of Acinetobacter baumannii. Biofouling 2014;30:965–73. https://doi.org/10.1080/08927014.2014.959941.

[83] Chen F ping, Kong N qing, Wang L, Luo Z, Yin J, Chen Y. Nanocomplexation between thymol and soy protein isolate and its improvements on stability and antibacterial properties of thymol. Food Chemistry 2021;334:127594. https://doi.org/10.1016/j.foodchem.2020.127594.

[84] Bugatti V, Brachi P, Viscusi G, Gorrasi G. Valorization of tomato processing residues through the production of active bio-composites for packaging applications. Frontiers in Materials 2019;6:1–10. https://doi.org/10.3389/fmats.2019.00034.

[85] Samsi MS, Kamari A, Sunradi IF, Yusoff SNM. SYNTHESIS , CHARACTERISATION AND APPLICATION OF GELATIN- SYNTHESIS , CHARACTERISATION AND APPLICATION OF GELATIN-CHITOSAN BLEND FILMS FOR. Fresenius Environmental Bulletin 2019;28:30–43.

[86] Jahit IS, Nazmi NNM, Isa MIN, Sorbon NM. Preparation and physical properties of gelatin / CMC / chitosan composite films as affected by drying temperature. International Food Research Journal 2016;23:1068–74.

[87] Pereda M, Ponce AG, Marcovich NE, Ruseckaite RA, Martucci JF. Chitosan-gelatin composites and bi-layer films with potential antimicrobial activity. Food Hydrocolloids 2011;25:1372–81. https://doi.org/10.1016/j.foodhyd.2011.01.001.

[88] Rujitanaroj P on, Pimpha N, Supaphol P. Wound-dressing materials with antibacterial activity from electrospun gelatin fiber mats containing silver nanoparticles. Polymer 2008;49:4723–32. https://doi.org/10.1016/j.polymer.2008.08.021.

[89] Gómez-Estaca J, López de Lacey A, López-Caballero ME, Gómez-Guillén MC, Montero P. Biodegradable gelatin-chitosan films incorporated with essential oils as antimicrobial agents for fish preservation. Food Microbiology 2010;27:889–96. https://doi.org/10.1016/j.fm.2010.05.012.

[90] Vinklárková L, Masteiková R, Foltýnová G, Muselík J, Pavloková S, Bernatonienė J, et al. Film wound dressing with local anesthetic based on insoluble carboxymethycellulose matrix. Journal of Applied Biomedicine 2017;15:313–20. https://doi.org/10.1016/j.jab.2017.08.002.

[91] Morgado PI, Aguiar-Ricardo A, Correia IJ. Asymmetric membranes as ideal wound dressings: An overview on production methods, structure, properties and performance relationship. Journal of Membrane Science 2015;490:139–51. https://doi.org/10.1016/j.memsci.2015.04.064.

[92] Wang J, Zheng X, Wu H, Zheng B, Jiang Z, Hao X, et al. Effect of zeolites on chitosan/zeolite hybrid membranes for direct methanol fuel cell. Journal of Power Sources 2008;178:9–19. https://doi.org/10.1016/j.jpowsour.2007.12.063.

[93] Chem JM, Jana S, Florczyk SJ, Leung M, Zhang M. High-strength pristine porous chitosan scaffolds for tissue engineering. Journal of Materials Chemistry 2012;22:6291–9. https://doi.org/10.1039/c2jm16676c.

[94] Mousavi Z, Naseri M, Babaei S, Mohammad S, Hosseini H, Shahram S. The effect of cross-linker type on structural , antimicrobial and controlled release properties of fi sh gelatin-chitosan composite fi lms incorporated with ε -poly- L -lysine. International Journal of Biological Macromolecules 2021;183:1743–52. https://doi.org/10.1016/j.ijbiomac.2021.05.159.

[95] Li Y, Tang C, He Q. Effect of orange (Citrus sinensis L .) peel essential oil on characteristics of blend films based on chitosan and fish skin gelatin. Food Bioscience 2021;41:100927. https://doi.org/10.1016/j.fbio.2021.100927.

[96] Fakhreddin S, Rezaei M, Zandi M, Farahmandghavi F. Development of bioactive fish gelatin / chitosan nanoparticles composite films with antimicrobial properties. FOOD CHEMISTRY 2016;194:1266–74. https://doi.org/10.1016/j.foodchem.2015.09.004.

[97] Wang H, Ding F, Ma L, Zhang Y. Edible films from chitosan-gelatin : Physical properties and food packaging application. Food Bioscience 2021;40:100871. https://doi.org/10.1016/j.fbio.2020.100871.